DALTON

Covalency in metal complexes of 1,4-diazabutadiene (dab). A density functional investigation of the electronic structures of $[M(dab)_2]$ (M = Li, Ga or Co) and $[Th(NH_3)(NH_2)_3(dab)]$*

Nikolas Kaltsoyannis

Department of Chemistry, University College London, 20 Gordon Street, London WC1H 0AJ, UK

Density functional methods have been used to investigate the valence electronic structures of four complexes containing 1,4-diazabutadiene (dab) ligands. One compound was chosen from each of the four 'blocks' of the Periodic Table, *viz*. $[Li(dab)_2]$, $[Ga(dab)_2]$, $[Co(dab)_2]$ and $[Th(dab)(NH_3)(NH_2)_3]$. The well documented structural differences between the two ligand rings of $[Ga(dbdab)_2]$ (dbdab = $Bu^tNCHCHNBu^t$) are interpreted in terms of a Jahn–Teller distortion arising from the partial occupation of the 7e highest occupied molecular orbital of the (hypothetical) molecule in which both rings are equivalent. This distortion brings about unequal occupancy of the dab π_3-localised molecular orbitals, with one ring becoming singly reduced and the other doubly reduced. The molecular orbital containing the single π_3 electron of the uninegative ring has a more negative eigenvalue than that containing the two electrons of the dianionic ring. While this runs contrary to the Aufbau principle, it provides a simple explanation of the 2:1 intensity ratio of the first two bands in the photoelectron spectrum of $[Ga(dbdab)_2]$. A similar effect is observed for $[Li(dab)_2]$. An analysis of the metal–dab bonding in all four compounds suggests predominantly ionic interactions in $[Li(dab)_2]$ and $[Th(dab)(NH_3)(NH_2)_3]$, with much greater covalency in $[Co(dab)_2]$. The conclusion for $[Ga(dab)_2]$ is less clear cut, being dependent on the method used to gauge covalency/ionicity.

1,4-Diazabutadiene (1,2-diiminoethane) (dab) forms complexes with metals from all areas of the Periodic Table. The energetic proximity of the valence molecular orbitals (MOs) of dab to the valence atomic orbitals (AOs) of the metals means that the bonding in dab complexes is extremely sensitive to factors such as the oxidation state of the metal, the nature of its valence AOs and the number and nature of any ancillary ligands. The electronic properties of dab derivatives of s-, p-, d- and f-block elements have been investigated by a variety of techniques including photoelectron spectroscopy (PES),[1] ESR [2–4] and electrochemistry,[4] and there has been some debate over electron localisation in such complexes. Electrochemical evidence has recently been used to suggest that ionic bonding predominates in s-block dab compounds and in the only dab derivative of an actinide element, $[Th(dbdab)\{N[CH_2CH_2N(SiMe_3)]_3\}]$ (dbdab = $Bu^tNCHCHNBu^t$), in contrast to more covalent bonding in p- and d-block dab compounds.[4] It was therefore decided to undertake a computational study of the electronic structure of representative dab complexes of the s, p, d and f elements, with a view to gaining further insight into this fascinating series and thus to evaluate the above hypothesis.

The simplest possible dab molecule, HNCHCHNH, was chosen as the ligand in all four compounds studied. These were $[Li(dab)_2]$, $[Ga(dab)_2]$, $[Co(dab)_2]$ and $[Th(dab)(NH_3)(NH_2)_3]$ as a model for $[Th(dbdab)\{N[CH_2CH_2N(SiMe_3)]_3\}]$. Structural data are available for dab derivatives of all four metals. Density functional theory[5] was selected as the calculational method as it has frequently been shown to yield accurate results on transition-metal and f-element compounds while retaining computational feasibility.[6] One particular advantage of the Amsterdam Density Functional[7,8] (ADF) program used in this study is its fragment-based approach, which allows molecular electronic structure to be analysed in terms of the interactions of specific fragments.

Computation

All calculations were performed using the ADF program suite.[9] Triple-zeta Slater-type orbital atomic basis sets were employed for all orbitals. Frozen cores were used for all elements bar H; C (1s), N (1s), Li (1s), Ga (3p), Co (3p) and Th (5d). A single polarisation function was included for all atoms except Th. The local density functional of Vosko *et al.*[10] was employed, with Stoll's correlation correction[11] and Becke's gradient correction[12] to the exchange part of the potential. Quasi-relativistic scalar corrections, Darwin and mass-velocity, were included for $[Th(dab)(NH_3)(NH_2)_3]$ *via* the Pauli formalism, in which the first-order scalar relativistic Pauli Hamiltonian is diagonalised in the space of the non-relativistic basis sets. Relativistic core potentials were computed for Th, C and N using the ADF auxiliary program DIRAC. Mulliken population analyses[13] were performed.

Molecular geometries were based upon the experimental data available for closely related compounds; $[Ga(dab)_2]$ upon $[Ga(dbdab)_2]$,[14] $[Li(dab)_2]$ upon $[Li(dbdab)_2]$,[3] $[Co(dab)_2]$ upon $[Co(dbdab)_2]$[15] and $[Th(dab)(NH_3)(NH_2)_3]$ upon $[Th(dbdab)\{N[CH_2CH_2N(SiMe_3)]_3\}]$.[4]

Results and Discussion

The computational results are presented as follows. The orbitals of dab which may become involved in bonding to a metal are briefly reviewed. Subsequently the electronic structure of $[Ga(dab)_2]$ is discussed, with emphasis on the relationship of the present results to the available crystallographic and PES data. The electronic structures of $[Li(dab)_2]$, $[Co(dab)_2]$ and $[Th(dab)(NH_3)(NH_2)_3]$ are then presented. Finally the nature of the metal–ligand bonding in all four molecules is explored.

HNCHCHNH

The valence MOs of HNCHCHNH are given in Table 1, and contour plots of the most important are shown in Fig. 1. There

---

* *Non-SI unit employed:* eV ≈ 1.6×10^{-19} J.

Table 1 Valence molecular orbital eigenvalues, occupations and compositions for HNCHCHNH

Orbital	Eigenvalue (eV)	Occupation	Fragment contribution (%) N	C	H
$2a_2$ (π_4)	+0.440	0	27 p_y	70 p_y	
$2b_1$ (π_3)	−3.367	0	65 p_y	31 p_y	2 p_y
$4b_2$ (n_-)	−5.463	2	54 p_z, 17 p_x, 12 s	3 p_z, 1 p_x	11 s
$5a_1$ (n_+)	−6.144	2	41 p_z, 22 p_x, 13 s	4 p_z, 1 p_x, 1 s	15 s
$1a_2$ (π_2)	−6.506	2	72 p_y	23 p_y	3 p_y
$1b_1$ (π_1)	−8.956	2	33 p_y	67 p_y	
$4a_1$	−10.631	2	20 p_z, 6 p_x	54 p_x	20 s
$3b_2$	−10.871	2	5 p_z, 25 p_x, 2 s	28 p_z	40 s

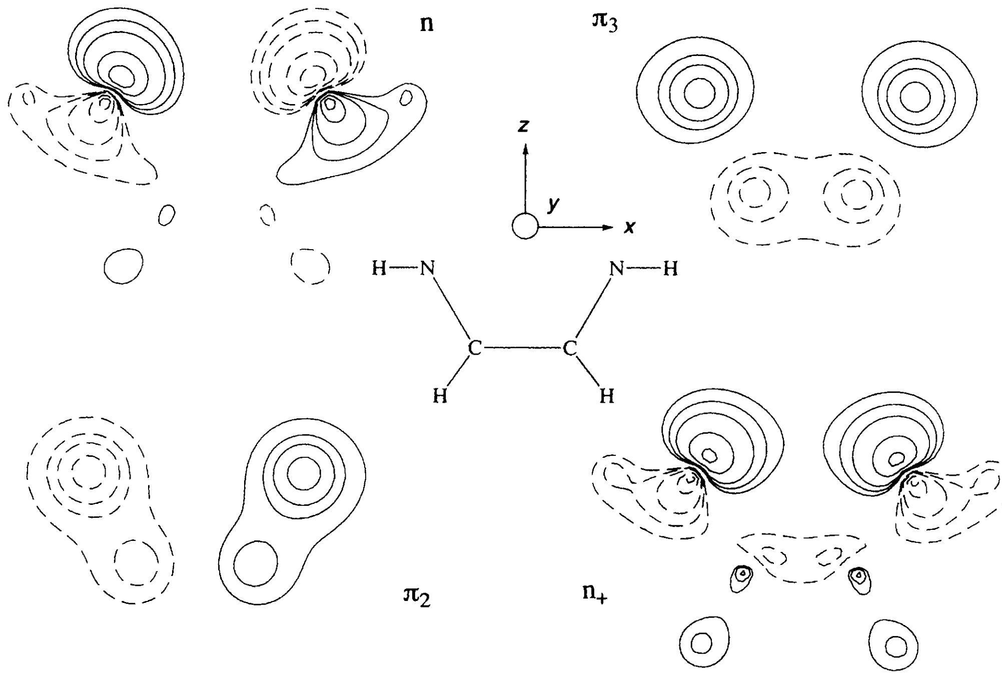

Fig. 1 Molecular orbital contour plots of the π_2, n_+, n_- and π_3 orbitals of HNCHCHNH. The π orbitals are viewed in a plane 0.4 Å above the molecular plane (the *xz* plane) while the n_+ and n_- orbitals are viewed in the molecular plane

are four π orbitals, π_1–π_4, formed from the carbon and nitrogen 2p AOs which lie perpendicular to the molecular plane: π_1 and π_2 are occupied in free dab, while π_3 is the lowest unoccupied molecular orbital (LUMO); π_1 and π_4 are localised mainly on the C atoms, with π_2 and π_3 being more N-based. In addition there are two σ orbitals, n_+ and n_-, which lie in the molecular plane.

[Ga(dab)$_2$]

The electronic structure of [Ga(dbdab)$_2$] has been the subject of a number of papers in recent years,[1,2,14] with the debate centring on the oxidation state of the metal. Although initially described as a gallium(II) complex,[14] it is now generally accepted that it is a gallium(III) compound. The two dbdab ligands have rather different structural parameters, and it has been suggested that one ring is singly reduced while the other carries a 2− formal charge.[2] These structural differences are frozen on the time-scale of X-ray crystallography, but the room-temperature ESR observation of the complex's single unpaired electron coupling to all four N atoms suggests that it is hopping from one ligand to the other on the time-scale of this experiment.

Such a structural distortion may be understood with reference to the electronic structure of a (hypothetical) [Ga(dab)$_2$] complex in which both rings have the same bond lengths and angles. This molecule would have D_{2d} symmetry, with a pseudo-tetrahedral disposition of N atoms about the metal. The results of a calculation of [Ga(dab)$_2$] using structural parameters averaged over the crystallographic data for both rings of [Ga(dbdab)$_2$] are given in Table 2 and on the left-hand side of Fig. 2. It is clear that the molecule is set up to undergo a Jahn–Teller distortion, given its partially filled e symmetry highest occupied molecular orbital (HOMO).

It is this Jahn–Teller mechanism which is believed to be the reason for the structural differences between the two ligands of [Ga(dbdab)$_2$]. Table 3 and Fig. 2 present the calculational results for [Ga(dab)$_2$] with different rings (now in C_{2v} symmetry) and it is clear that there is a pronounced splitting of the 7e HOMO of the undistorted molecule. This orbital is made up almost entirely of the π_3 orbital of the dab ligands (Table 2) and this composition carries through to the $7b_2$ and $7b_1$ MOs of the distorted structure. The unequal occupancy of the $7b_2$ and $7b_1$ orbitals may therefore be described as the π_3 orbital of one dab ring (A) containing two electrons, with only one electron in the equivalent orbital of the other ring (B). This elegantly rationalises the observed structural parameters. As may be seen from Fig. 1, π_3 is C–C bonding and C–N antibonding. Ring A has shorter C–C and longer C–N distances than its singly reduced partner.

The compound [Ga(dab)$_2$] has a single unpaired electron, and it is therefore best to address its electronic structure through the use of spin-unrestricted calculations (in which electrons of the same symmetry but different spins are not

Table 2 Valence molecular orbital eigenvalues, occupations and compositions for [Ga(dab)$_2$], idealised to D_{2d} symmetry with equivalent dab rings

			Fragment contribution (%)	
Orbital	Eigenvalue (eV)	Occupation	Ga	dab
7e	−2.965	3	4 p	92 2b$_1$ (π_3), 2 4b$_2$
1a$_2$	−6.071	2		100 1a$_2$ (π_2)
2b$_1$	−6.270	2	2 d	97 1a$_2$ (π_2)
6e	−7.182	4	8 p	72 4b$_2$ (n$_-$), 13 1b$_1$, 3 3b$_2$
6b$_2$	−7.554	2	10 p	5 4a$_1$, 78 5a$_1$ (n$_+$), 4 3a$_1$
5e	−8.422	4	3 p	83 1b$_1$ (π_1), 9 4b$_2$, 2 2b$_1$
6a$_1$	−8.923	2	9 s	4 3a$_1$, 55 4a$_1$, 31 5a$_1$ (n$_+$)

Table 3 Valence molecular orbital eigenvalues, occupations and compositions for [Ga(dab)$_2$], with C_{2v} symmetry and inequivalent dab rings. Ring A is formally doubly reduced and ring B singly reduced

			Fragment contribution (%)		
Orbital	Eigenvalue (eV)	Occupation	Ga	dab (A)	dab (B)
7b$_1$	−2.302	2	7 p	4 1b$_1$ (π_1), 87 2b$_1$ (π_3)	2 4b$_2$ (n$_-$)
7b$_2$	−3.693	1	2 p	3 4b$_2$ (n$_-$)	93 2b$_1$ (π_3)
3a$_2$	−5.128	2		98 1a$_2$ (π_2)	
6b$_2$	−6.674	2	12 p	5 3b$_2$, 74 4b$_2$ (n$_-$)	3 1b$_1$ (π_1), 2 2b$_1$ (π_3)
6b$_1$	−7.017	2	2 d	81 1b$_1$ (π_1)	15 4b$_2$ (n$_-$)
2a$_2$	−7.325	2			99 1a$_2$ (π_2)
12a$_1$	−7.383	2	7 p, 2 s	5 3a$_1$, 13 4a$_1$, 49 5a$_1$ (n$_+$)	19 5a$_1$ (n$_+$)
5b$_1$	−8.168	2	9 p	13 1b$_1$ (π_1), 2 2b$_1$ (π_3)	2 3b$_2$, 71 4b$_2$ (n$_-$)
11a$_1$	−8.655	2	2 p	67 3a$_1$	3 4a$_1$, 23 5a$_1$ (n$_+$)
5b$_2$	−9.334	2	2 d	64 3b$_2$	32 1b$_1$ (π_1)
4b$_2$	−9.577	2	1 p	29 3b$_2$, 4 4b$_2$ (n$_-$)	63 1b$_1$ (π_1)
10a$_1$	−9.864	2	11 s	2 1a$_1$, 6 2a$_1$, 17 3a$_1$, 14 4a$_1$	2 3a$_1$, 28 4a$_1$, 20 5a$_1$ (n$_+$)

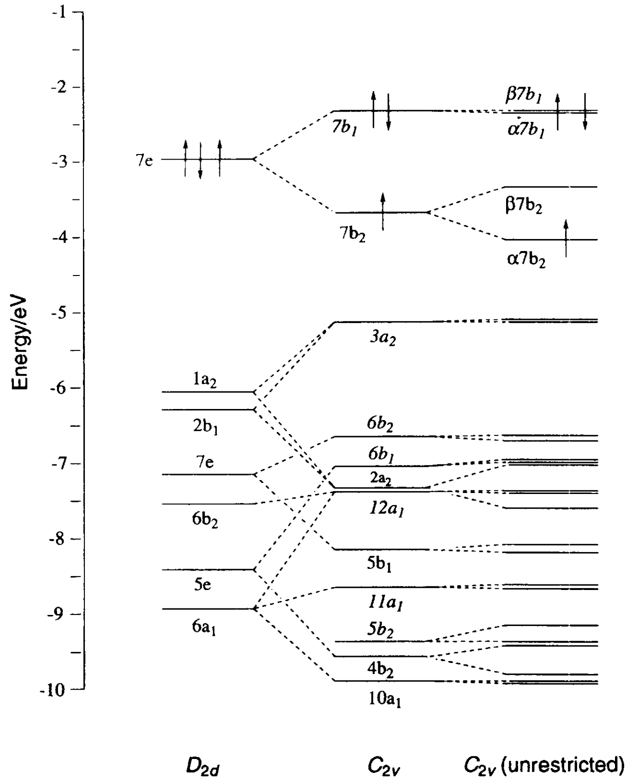

Fig. 2 Molecular orbital energy-level diagram for [Ga(dab)$_2$] with (*a*) equivalent ligands (D_{2d} symmetry), (*b*) inequivalent ligands (C_{2v} symmetry) and (*c*) inequivalent ligands (C_{2v} symmetry) and no spin restriction. In the C_{2v} calculations the italicised orbitals are localised predominantly on the more reduced dab (ring A). Most of the symmetry labels have been omitted from the unrestricted calculation for clarity

constrained to have the same spatial wavefunction). Table 4 and Fig. 2 present the results of an unrestricted calculation on the distorted, C_{2v}, structure of [Ga(dab)$_2$]. There are generally only small differences between these results and those from the restricted calculation, although the single electron in the restricted 7b$_2$ MO is stabilised significantly in the unrestricted calculation. In both cases the MOs with more negative eigenvalues are generally localised predominantly on ring B, with those closer to the HOMO being largely based on ring A. The relative energies of the equivalent fragment orbitals of rings A and B reflect the respective charges on the two ligands.

The occupations of the highest occupied orbitals of the distorted structure are of interest. In both the restricted and unrestricted cases the single electron in the MO formed predominantly from the π_3 orbital of ring B, the 7b$_2$ orbital, is more stable than the two electrons in the 7b$_1$ HOMO. Thus the Aufbau principle[16] is not obeyed in this case. This is particularly relevant to the photoelectron spectrum of [Ga(dbdab)$_2$],[1] which has a 2:1 relative intensity for the first two bands. The assignment of these bands equates the first (of lowest ionisation energy) with molecular ions having the (dab A π_3)^1 (dab B π_3)^1 electronic configuration and the second (of half the intensity) with the (dab A π_3)^2 configuration. It was suggested that a 'naive application of Koopmans' theorem with neglect of any electron repulsion considerations' could not explain the relative intensity of the first two bands, and a more complicated rationale was used. The results of the calculations presented here, however, are entirely consistent with a simple Koopmans approach,* the relative intensities of the first two bands reflecting the relative populations of the 7b$_1$ and 7b$_2$ MOs. Regardless of the reasoning employed, both approaches yield the same assignment for the molecular ion states represented by the first two PE bands and agree that oxidation of [Ga(dab)$_2$] should result in a cation with two singly reduced ligands and a triplet ground state.

---

* Strictly speaking, Koopmans' theorem cannot be applied to ground-state density functional eigenvalues.[17] Transition-state[17] calculations on the 7b$_1$ and 7b$_2$ MOs, however, yield the same orbital ordering and energy separations as those from the ground-state calculations.

Table 4 Unrestricted valence molecular orbital eigenvalues, occupations and compositions for [Ga(dab)$_2$], with C_{2v} symmetry and inequivalent dab rings. Ring A is formally doubly reduced and ring B singly reduced

				Fragment contribution (%)		
Orbital	Spin	Eigenvalue (eV)	Occupation	Ga	dab (A)	dab (B)
$7b_1$	β	−2.291	1	7 p	4 $1b_1$ (π_1), 87 $2b_1$ (π_3)	
$7b_1$	α	−2.299	1	7 p	4 $1b_1$ (π_1), 87 $2b_1$ (π_3)	
$7b_2$	β	−3.321	0	2 p	3 $4b_2$ (n_-)	93 $2b_1$ (π_3)
$7b_2$	α	−4.024	1	1 p	4 $4b_2$ (n_-)	93 $2b_1$ (π_3)
$3a_2$	β	−5.116	1		98 $1a_2$ (π_2)	
$3a_2$	α	−5.124	1		98 $1a_2$ (π_2)	
$6b_2$	β	−6.639	1	11 p	3 $2b_2$, 5 $3b_2$, 74 $4b_2$ (n_-)	3 $1b_1$ (π_1), 1 $2b_1$ (π_3)
$6b_2$	α	−6.693	1	12 p	2 $2b_2$, 5 $3b_2$, 74 $4b_2$ (n_-)	2 $1b_1$ (π_1), 2 $2b_1$ (π_3)
$6b_1$	β	−6.995	1	2 d	79 $1b_1$ (π_1)	16 $4b_2$ (n_-)
$2a_2$	β	−7.000	1			99 $1a_2$ (π_2)
$6b_1$	α	−7.024	1	2 d	82 $1b_1$ (π_1)	13 $4b_2$ (n_-)
$12a_1$	β	−7.352	1	7 p, 2 s	5 $3a_1$, 12 $4a_1$, 49 $5a_1$ (n_+)	20 $5a_1$ (n_+)
$12a_1$	α	−7.397	1	7 p, 2 s	5 $3a_1$, 14 $4a_1$, 49 $5a_1$ (n_+)	19 $5a_1$ (n_+)
$2a_2$	α	−7.615	1			99 $1a_2$ (π_2)
$5b_1$	β	−8.108	1	10 p	15 $1b_1$	69 $4b_2$ (n_-)
$5b_1$	α	−8.216	1	10 p	12 $1b_1$	72 $4b_2$ (n_-)
$11a_1$	β	−8.627	1	2 p, 1 s	67 $4a_1$	3 $4a_1$, 23 $5a_1$ (n_+)
$11a_1$	α	−8.670	1	2 p, 1 s	67 $4a_1$	3 $4a_1$, 23 $5a_1$ (n_+)
$5b_2$	β	−9.145	1		81 $3b_2$	16 $1b_1$ (π_1)
$5b_2$	α	−9.375	1		87 $3b_2$, 3 $4b_2$ (n_-)	7 $1b_1$ (π_1)
$4b_2$	β	−9.440	1		14 $3b_2$	77 $1b_1$ (π_1), 6 $2b_1$ (π_3)
$4b_2$	α	−9.775	1		7 $3b_2$, 3 $4b_2$ (n_-)	88 $1b_1$ (π_1)
$10a_1$	β	−9.827	1	11 s	6 $3a_1$, 17 $4a_1$, 13 $5a_1$ (n_+)	2 $3a_1$, 28 $4a_1$, 19 $5a_1$ (n_+)
$10a_1$	α	−9.888	1	11 s	6 $3a_1$, 16 $4a_1$, 13 $5a_1$ (n_+)	2 $3a_1$, 27 $4a_1$, 21 $5a_1$ (n_+)

Table 5 Unrestricted valence molecular orbital eigenvalues, occupations and compositions for [Li(dab)], with C_{2v} symmetry and inequivalent dab rings. Ring A is formally singly reduced and ring B neutral

				Fragment contribution (%)		
Orbital	Spin	Eigenvalue (eV)	Occupation	Li	dab (A)	dab (B)
$6b_1$	β	−0.921	0	4 p	95 $2b_1$ (π_3)	
$6b_1$	α	−1.624	1	3 p	96 $2b_1$ (π_3)	
$6b_2$	β	−3.373	0		3 $4b_2$ (n_-)	97 $2b_1$ (π_3)
$6b_2$	α	−3.375	0		2 $4b_2$ (n_-)	98 $2b_1$ (π_3)
$2a_2$	β	−4.610	1		100 $1a_2$ (π_2)	
$5b_2$	β	−4.646	1	9 p	88 $4b_2$ (n_-)	2 $2b_1$ (π_3)
$10a_1$	β	−4.794	1	6 s	90 $5a_1$ (n_+)	
$5b_2$	α	−4.797	1	8 p	89 $4b_2$ (n_-)	2 $2b_1$ (π_3)
$10a_1$	α	−4.944	1	6 s	90 $5a_1$ (n_+)	
$2a_2$	α	−5.228	1		100 $1a_2$ (π_2)	
$5b_1$	β	−6.707	1	1 d	91 $1b_1$ (π_1)	8 $4b_2$ (n_-)
$9a_1$	β	−7.029	1	3 p		95 $5a_1$ (n_+)
$9a_1$	α	−7.032	1	3 p		95 $5a_1$ (n_+)
$5b_1$	α	−7.042	1	1 p, 1 d	16 $1b_1$ (π_1)	82 $1a_2$ (π_2)
$4b_1$	β	−7.114	1	4 p	7 $1b_1$ (π_1)	89 $4b_2$ (n_-)
$4b_1$	α	−7.338	1	3 p	83 $1b_1$ (π_1)	14 $4b_2$ (n_-)
$1a_2$	β	−8.225	1			100 $1a_2$ (π_2)
$1a_2$	α	−8.225	1			100 $1a_2$ (π_2)
$8a_1$	β	−8.711	1		98 $4a_1$	
$8a_1$	α	−8.833	1		98 $4a_1$	
$4b_2$	β	−9.194	1		100 $3b_2$	
$4b_2$	α	−9.279	1		100 $3b_2$	
$3b_2$	α	−10.093	1	11 s		100 $1b_1$ (π_1)
$3b_2$	β	−10.096	1	11 s		100 $1b_1$ (π_1)

[Li(dab)$_2$]

The synthesis and characterisation of [Li(dbdab)$_2$] has recently been reported.[3] Its structure is similar to that of [Ga(dbdab)$_2$]: C_{2v} symmetry with two ligands of differing bond lengths and angles. The structural data are consistent with one ring being singly reduced and the other formally neutral.

Table 5 presents the results of an unrestricted calculation on [Li(dab)$_2$], based on the structural parameters of [Li(dbdab)$_2$]. As with the gallium analogue, there is unequal occupation of the MOs composed of the π_3 levels of the dab rings ($6b_2$ and $6b_1$). In this case the π_3 orbitals of the neutral ring are unoccupied, while those of the uninegative ligand contain one electron (α $6b_1$). Once again the π_3 orbitals of the less-reduced ligand have more negative eigenvalues than those of the more reduced ligand, yet contain fewer electrons (in this case none). The trapping of the unpaired electron on one of the rings clearly produces an electronic structure in violation of the Aufbau principle.

[Co(dab)$_2$]

Although there are minor structural differences between the two rings of [Co(dbdab)$_2$][15] these are sufficiently small so as

Table 6 Valence molecular orbital eigenvalues, occupations and compositions for $[Co(dab)_2]$

Orbital	Eigenvalue (eV)	Occupation	Fragment contribution (%)	
			Co	dab
7e	−1.965	0	37 d	51 $2b_1$ (π_3), 12 $1b_1$ (π_1)
6e	−3.507	4	33 d, 5 p	11 $4b_2$ (n_-), 46 $2b_1$ (π_3), 4 $1b_1$ (π_1)
$6b_2$	−3.656	1	81 d, 4 p	13 $5a_1$ (n_+)
$2b_1$	−3.959	2	83 d	16 $1a_2$ (π_2)
$6a_1$	−4.327	2	92 d, 4 s	1 $4a_1$, 1 $3a_1$
$1a_2$	−6.326	2		100 $1a_2$ (π_2)
$1b_1$	−6.849	2	16 d	83 $1a_2$ (π_2)
5e	−7.131	4	3 p, 21 d	66 $4b_2$ (n_-), 1 $1b_1$ (π_1), 4 $3b_2$
$5a_1$	−7.851	2	7 s, 2 d	3 $3a_1$, 13 $4a_1$, 74 $5a_1$ (n_+)
$5b_2$	−10.073	2	4 p, 14 d	5 $4a_1$, 73 $5a_1$ (n_+)
$4a_1$	−10.348	2	4 s	85 $4a_1$, 9 $5a_1$ (n_+)
4e	−10.660	4	4 d	92 $1b_1$ (π_1), 1 $3b_2$, 1 $4b_2$ (n_-)

Table 7 Unrestricted valence molecular orbital eigenvalues, occupations and compositions for $[Co(dab)_2]$

Orbital	Spin	Eigenvalue (eV)	Occupation	Fragment contribution (%)	
				Co	dab
7e	β	−1.503	0	58 d	26 $2b_1$ (π_3), 14 $4b_2$ (n_-)
7e	α	−2.128	0	16 d	76 $2b_1$ (π_3), 7 $4b_2$ (n_-)
$6b_2$	β	−2.500	0	86 d, 4 s	7 $5a_1$, (n_+)
6e	β	−3.359	2	18 d, 4 p	71 $2b_1$, (π_3), 4 $4b_2$ (n_-)
$2b_1$	β	−3.782	1	85 d	14 $1a_2$ (π_2)
6e	α	−3.987	2	45 d, 6 p	24 $4b_2$ (n_-), 20 $2b_1$ (π_3), 5 $1b_1$ (π_3)
$6a_1$	β	−3.976	1	92 d, 4 s	1 $3a_1$, 1 $5a_1$ (n_+)
$2b_1$	α	−4.376	1	76 d	24 $1a_2$ (π_2)
$6b_2$	α	−4.799	1	66 d, 6 s	26 $5a_1$ (n_+)
$6a_1$	α	−4.848	1	92 d, 4 s	1 $3a_1$, 1 $4a_1$, 2 $5a_1$ (n_+)
$1a_2$	α	−6.135	1		100 $1a_2$ (π_2)
$1a_2$	β	−6.433	1		100 $1a_2$ (π_2)
$1b_1$	α	−6.786	1	24 d	76 $1a_2$ (π_2)
$1b_1$	β	−6.921	1	14 d	86 $1a_2$ (π_2)
$5b_2$	β	−7.000	1	5 p, 8 d	1 $3a_1$, 4 $4a_1$, 79 $5a_1$ (n_+)
$5b_2$	α	−7.363	1	3 p, 28 d	8 $4a_1$, 58 $5a_1$ (n_+)
5e	β	−7.440	2	3 p, 17 d	72 $4b_2$ (n_-), 3 $3b_2$
5e	α	−7.776	2	3 p, 35 d	55 $4b_2$ (n_-), 3 $3b_2$
$5a_1$	β	−7.819	1	7 s, 3 d	2 $3a_1$, 12 $4a_1$, 75 $5a_1$ (n_+)
$5a_1$	α	−7.877	1	7 s, 3 d	3 $3a_1$, 14 $4a_1$, 72 $5a_1$ (n_+)
4e	α	−8.477	2	10 d	83 $1b_1$ (π_1)
4e	β	−8.667	2	2 d, 1 p	95 $1b_1$ (π_1)

to permit study of $[Co(dab)_2]$ under D_{2d} symmetry, with two equivalent ligands. Tables 6 and 7 present the results of restricted and unrestricted calculations respectively for $[Co(dab)_2]$, and the energy levels are also shown in Fig. 3. With a pseudotetrahedral disposition of N atoms about the Co, the splitting of the MOs of predominant metal d-orbital character may be expected to resemble the familiar e-below-t_2 arrangement commonly found for tetrahedral transition-metal complexes.[16] Descent in symmetry from T_d to D_{2d} lifts the degeneracy of both e and t_2 irreducible representations, to $a_1 + b_1$ and $b_2 + e$ respectively. The spin-restricted (Table 6 and the left-hand side of Fig. 3) $6a_1$ and $2b_1$ MOs of $[Co(dab)_2]$ may therefore be associated with the e symmetry d-based orbitals of a tetrahedral transition-metal complex, although the situation for the t_2 levels is less clear. The $6b_2$ MO is largely cobalt d-based, but both the 6e and 7e orbitals are a mixture of metal d and dab π_3. It would appear that tetrahedral t_2(d) character is spread over both the 6e and the 7e MOs of $[Co(dab)_2]$, with the consequence that there is appreciable ligand character in what would simplistically be regarded as the cobalt 3d manifold.

As with $[Ga(dab)_2]$ and $[Li(dab)_2]$, the orbital occupation of $[Co(dab)_2]$ does not obey the Aufbau principle. The $6b_2$ d-based MO contains only one electron, even though it has a more negative eigenvalue than the filled 6e HOMO. It would appear to be more favourable to populate fully the MO with significant ligand π_3 character at the expense of the d-based $6b_2$ orbital.

There is a number of differences between the spin-restricted and -unrestricted calculations. Both the 4e (π_1-based) and the $5b_2$ (n_+-based) MOs are significantly destabilised. Interestingly, the α-spin orbitals gain metal d-orbital character with respect to the restricted orbitals, such that the composition of the α-spin 4e and $5b_2$ levels is different to their β-spin counterparts. Of the more metal-localised MOs, the α- and β-spin $6b_2$ orbitals are very widely separated energetically, with the β $6b_2$ remaining largely metal d-based but the α $6b_2$ acquiring greater ligand n_+ character. The α and β 6e orbitals also have significantly different compositions.

$[Th(dab)(NH_3)(NH_2)_3]$

Table 8 presents the results of a C_s symmetry, unrestricted calculation on $[Th(dab)(NH_3)(NH_2)_3]$, based on the crystal structure of $[Th(dbdab)\{N[CH_2CH_2N(SiMe_3)]_3\}]$.[4] Scalar relativistic effects have been included by use of relativistic frozen-core potentials for Th and (much less importantly) C and N. These corrections account for the relativistic modification of AO energies[18] but stop short of a fully relativistic treatment involving spin–orbit coupling and

Table 8 Unrestricted valence molecular orbital eigenvalues, occupations and compositions for [Th(dab)(NH$_3$)(NH$_2$)$_3$], with C_s symmetry

Orbital	Spin	Eigenvalue (eV)	Occupation	Fragment contribution (%) Th	(NH$_3$)(NH$_2$)$_3$	dab
20a′	β	−2.590	0	1 s, 4 d, 1 f		91 2b$_1$ (π$_3$)
20a′	α	−3.262	1	1 s, 2 d, 1 f		93 2b$_1$ (π$_3$)
12a″	β	−4.265	1	6 f	92 1a$_2$	
12a″	α	−4.268	1	6 f	92 1a$_2$	
11a″	β	−4.496	1	3 p, 9 d	21 4e, 66 5e	
11a″	α	−4.502	1	3 p, 9 d	21 4e, 66 5e	
19a′	β	−4.568	1	1 p, 10 d	15 4e, 72 5e	
19a′	α	−4.576	1	1 p, 10 d	15 4e, 72 5e	
10a″	β	−5.939	1	4 p, 9 d	35 4e, 15 5e	26 4b$_2$ (n$_-$), 7 1a$_2$ (π$_2$)
10a″	α	−6.000	1	3 p, 11 d, 2 f	39 4e, 16 5e	25 4b$_2$ (n$_-$), 2 1a$_2$ (π$_2$)
18a′	β	−6.011	1	2 p, 5 d, 3 f	8 4e, 23 4a$_1$	54 5a$_1$ (n$_+$)
18a′	α	−6.094	1	3 p, 5 d, 3 f	10 4e, 25 4a$_1$	47 5a$_1$ (n$_+$)
9a″	β	−6.402	1	3 d		4 4b$_2$ (n$_-$), 90 1a$_2$ (π$_2$)
17a′	α	−6.444	1	2 p, 17 d	54 4e, 11 5e, 7 4a$_1$	5 5a$_1$ (n$_+$)
17a′	β	−6.464	1	2 p, 17 d	54 4e, 12 5e, 5 4a$_1$	4 5a$_1$ (n$_+$)
16a′	β	−6.779	1	7 s, 1 d, 5 f	24 4a$_1$, 40 5a$_1$	19 5a$_1$ (n$_+$)
16a′	α	−6.813	1	7 s, 3 d, 2 f	19 4a$_1$, 42 5a$_1$	24 5a$_1$ (n$_+$)
9a″	α	−6.952	1	2 d		7 4b$_2$ (n$_-$), 89 1a$_2$ (π$_2$)
8a″	β	−7.055	1	15 d, 1 f	23 4e, 2 5e	53 4b$_2$ (n$_-$), 1 1a$_2$ (π$_2$)
8a″	α	−7.151	1	13 d, 1 f	19 4e, 2 5e	53 4b$_2$ (n$_-$), 7 1a$_2$ (π$_2$)
15a′	β	−7.780	1	4 s, 4 d	30 4a$_1$, 47 5a$_1$	10 5a$_1$
15a′	α	−7.797	1	5 s, 3 d	30 4a$_1$, 45 5a$_1$	12 5a$_1$
14a′	β	−8.823	1	2 d		97 1b$_1$ (π$_1$)
14a′	α	−8.877	1	1 d		98 1b$_1$ (π$_1$)

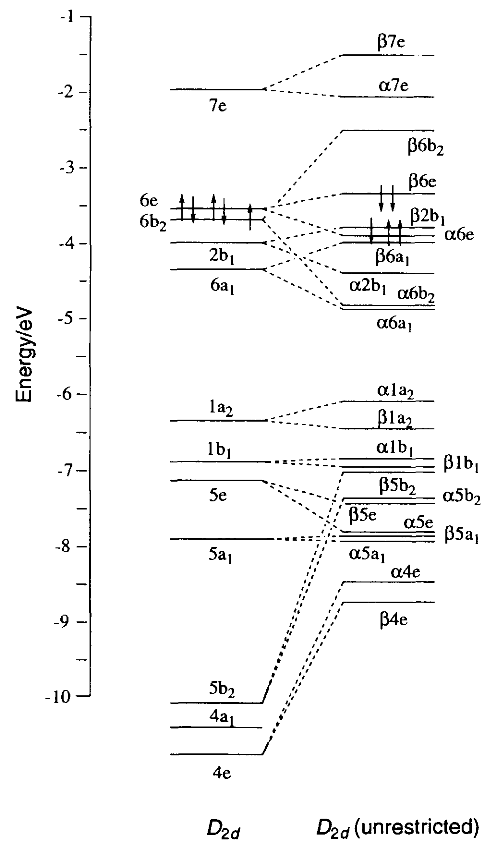

Fig. 3 Restricted and unrestricted molecular orbital energy-level diagram for [Co(dab)$_2$] with D_{2d} symmetry

molecular double point groups.[19] All of the valence orbitals of the (NH$_3$)(NH$_2$)$_3$ fragment referred to in Table 8 are predominantly localised on the N atoms of the NH$_2$ groups, with the exception of the NH$_3$-based 5a$_1$ orbital. Given that the focus of this study is the bonding between the Th and the dab ligand, the (NH$_3$)(NH$_2$)$_3$ fragment will not be discussed further.

The structural data available for [Th(dbdab){N[CH$_2$CH$_2$N(SiMe$_3$)]$_3$}] indicate that the dbdab fragment is best regarded as singly reduced,[4] in agreement with the Th being in the +4 oxidation state {the N[CH$_2$CH$_2$N(SiMe$_3$)]$_3$ fragment carries a formal 3− charge}. The cyclic voltammetry response of [Th(dbdab){N[CH$_2$CH$_2$(SiMe$_3$)]$_3$}] led the authors to conclude that it undergoes a chemically irreversible oxidation corresponding to the loss of the electron localised on the π$_3$ orbital of the dbdab fragment. This is entirely consistent with the calculational results, which indicate that the α 20a′ HOMO of [Th(dab)(NH$_3$)(NH$_2$)$_3$] has 93% dab π$_3$ character. In general, there is virtually no mixing of the dab π orbitals with the thorium valence AOs, as evidenced by the composition of the α and β 14a′ and α and β 9a″ MOs.

Estimates of covalency

There are several different ways in which Mulliken population analyses may be used to provide indications of the type of bonding between fragments within molecules. One of the simplest approaches is to identify one or two MOs present in all of the molecules under investigation and examine their composition in terms of the contributions from the molecular fragments. In the present study, the MOs in which the n$_+$ and n$_-$ orbitals of the dab fragments play a significant role lend themselves to such an analysis, as n$_+$ and n$_-$ are both spatially and energetically well disposed to interact with the metal atoms. Table 9 indicates the metal contributions to the relevant MOs of all four compounds studied; significant metal character in these levels suggests appreciable metal–dab covalency.

In the case of the MOs with predominant dab n$_-$ character, it is clear that the cobalt complex has the largest metal contribution. Next comes the thorium compound, although it is not clear from this simple analysis whether the 15% metal contribution is involved in Th–dab or Th–(NH$_3$)(NH$_2$)$_3$ bonding. Given the data from the other analyses (see above) it is very likely to be the latter. The compound [Ga(dab)$_2$] is next in line, with a *ca.* 11% gallium p contribution. Finally, the lithium complex has virtually no metal content in these MOs. A somewhat different situation is found in the compositions of

Table 9 Metal contributions (%) to the MOs (labels in parentheses) composed predominantly of dab n_- and n_+ for [Li(dab)$_2$], [Ga(dab)$_2$], [Co(dab)$_2$] and [Th(dab)(NH$_3$)(NH$_2$)$_3$]

		Li	Ga	Co	Th
n_-	(dab) A		11.5 p ($6b_2$)		
	(dab) B	3.5 p ($4b_1$)	10 p ($5b_1$)		
	dab			26 d, 3 p (5e)	14 d, 1 f (8a″)
n_+	(dab) A	6 s ($10a_1$)	7 p, 2 s ($12a_1$)		
	(dab) B	3 p ($9a_1$)			
	dab			7 s, 3 d ($5a_1$)	2.5 p, 5 d, 3 f (18a′)

Table 10 Metal–dab fragment overlap populations for [Li(dab)$_2$], [Ga(dab)$_2$], [Co(dab)$_2$] and [Th(dab)(NH$_3$)(NH$_2$)$_3$]

	Li	Ga	Co	Th
(dab) A	0.34	0.74		
(dab) B	0.14	0.34		
dab			1.22	0.32

Table 11 Fragment charges for [Li(dab)$_2$], [Ga(dab)$_2$], [Co(dab)$_2$] and [Th(dab)(NH$_3$)(NH$_2$)$_3$]

	Calculated charge	Formal charge	Calculated charge/ formal charge
Li	+0.391 3	+1	+0.391 3
(dab) A	−0.529 6		
(dab) B	+0.138 4		
Ga	+1.305 8	+3	+0.435 2
(dab) A	−0.943 0		
(dab) B	−0.363 0		
Co	+0.532 5	+2	+0.266 3
dab	−0.266 25		
Th	+2.138 4	+4	+0.534 6
dab	−0.661 4		
(NH$_3$)(NH$_2$)$_3$	−1.477 0		

the MOs based on the dab n_+ orbitals. In these cases the metal contributions are much more equal, at the 5–10% level. The conclusion from this MO composition analysis, therefore, is not definitive, but is inclined toward the cobalt complex having the greatest covalency and the lithium compound the least.

A more sophisticated approach is to examine the metal–dab fragment overlap populations. These are useful indications of the bonding/antibonding nature of the interaction between fragments, and consider all of the MOs (not just specific orbitals as was the case above). A positive overlap population indicates a bonding interaction and negative one an antibonding interaction. Increasing covalency is reflected in larger overlap populations. Table 10 gives the metal-dab fragment overlap populations of all four compounds, and is especially useful as the interaction within the Th–dab fragment has been separated from that of the Th–(NH$_3$)(NH$_2$)$_3$. There are significant differences between the complexes, with the +1.22 value for [Co(dab)$_2$] indicating that it has the most covalent metal–dab interaction; [Ga(dab)$_2$] occupies a clear second place, with the compounds of Li and Th having the least covalent interactions. In [Li(dab)$_2$] and [Ga(dab)$_2$] the greater overlap population between the metal and the more reduced dab ring reflects the formal transfer of more electron density from the metal to ring A than to B.

Large covalent interactions are likely to be accompanied by small charge separations within the molecules, while ionic bonding will be reflected in greater +/− charge differences. Table 11 presents the fragment charges for all four compounds, and the final column attempts to normalise the metal charge by dividing the calculated charge by the formal oxidation state. It is clear that the cobalt complex has the least ionic interaction and that of Th the largest, in agreement with the overlap-population data. The charge data differ from the overlap-population data in the case of the compounds of Li and Ga, however, with a rather greater calculated charge for the Ga than the Ga–dab overlap population might suggest.

In summary, the calculational data support the assertion of predominantly ionic metal–dab bonding in the s-block and Th–dab complexes, and of much greater covalency in the transition metals. The p-block example gives conflicting results: the overlap population suggests significant covalency and yet the calculated charges indicate appreciable electrostatic interaction.

Acknowledgements

I would like to thank Dr. Peter Scott for helpful discussions.

References

1 F. G. N. Cloke, C. I. Dalby, P. J. Daff and J. C. Green, *J. Chem. Soc., Dalton Trans.*, 1991, 181.
2 W. Kaim and W. Matheis, *J. Chem. Soc., Chem. Commun.*, 1991, 597.
3 M. G. Gardiner, G. R. Hanson, M. J. Henderson, F. C. Lee and C. L. Raston, *Inorg. Chem.*, 1994, **33**, 2456.
4 P. Scott and P. B. Hitchcock, *J. Chem. Soc., Chem. Commun.*, 1995, 579.
5 R. G. Parr and W. Yang, *Density-functional Theory of Atoms and Molecules*, Oxford University Press, New York, 1989.
6 *Density Functional Methods in Chemistry*, eds. J. K. Labanowski and J. W. Andzelm, Springer, New York, 1991.
7 E. J. Baerends, D. E. Ellis and P. Ros, *Chem. Phys.*, 1973, **2**, 41.
8 G. te Velde and E. J. Baerends, *J. Comput. Phys.*, 1992, **99**, 84.
9 ADF⟨1.1.4⟩, Department of Theoretical Chemistry, Vrije Universiteit, Amsterdam, 1995.
10 S. H. Vosko, L. Wilk and M. Nusair, *Can. J. Phys.*, 1980, **58**, 1200.
11 H. Stoll, C. M. E. Pavlidou and H. Preuss, *Theor. Chim. Acta*, 1978, **49**, 143.
12 A. Becke, *Phys. Rev. A*, 1988, **38**, 3098.
13 R. S. Mulliken, *J. Chem. Phys.*, 1955, **23**, 1833.
14 F. G. N. Cloke, G. R. Hanson, M. J. Henderson, P. B. Hitchcock and C. L. Raston, *J. Chem. Soc., Chem. Commun.*, 1989, 1002.
15 P. J. Daff, Part II Thesis, Oxford University, 1990.
16 D. F. Shriver, P. W. Atkins and C. H. Langford, *Inorganic Chemistry*, 2nd edn., Oxford University Press, Oxford, 1994.
17 J. S. Slater, *The Calculation of Molecular Orbitals*, Wiley, New York, 1979.
18 P. Pyykkö, *Acc. Chem. Res.*, 1979, **8**, 276.
19 N. Kaltsoyannis and B. E. Bursten, *Inorg. Chem.*, 1995, **34**, 2735.

Received 31*st October* 1995; *Paper* 5/07176C